Simultaneous normal and parallel incidence planar left-handed metamaterial

Jianhong Lv,[1,*] Baorong Yan,[1] Minghai Liu,[1] and Xiwei Hu[1,2,†]
[1]*College of Electrical and Electronic Engineering, Huazhong University of Science and Technology, Wuhan 430074, People's Republic of China*
[2]*College of Physics, Huazhong University of Science and Technology, Wuhan 430074, People's Republic of China*
(Received 26 March 2009; revised manuscript received 17 June 2009; published 21 August 2009)

We investigate numerically the negative refraction of a simultaneous normal and parallel incidence planar left-handed metamaterial (LHM) in this paper. This LHM is comprised of fourfold C-shaped rings, which are printed on both sides of the substrates symmetrically, and it can exhibit left-handed properties with electromagnetic wave incident in three different directions. The retrieved result and the simulated result verify the left-handed properties of the fourfold C-shaped metamaterial very well. Then the different electric responses of the normal and parallel incidence cases to the incident electromagnetic wave are discussed, and it is due to the different distribution of the induced currents in the metallic wires.

DOI: 10.1103/PhysRevE.80.026605 PACS number(s): 41.20.Jb, 78.20.Ci, 42.25.Bs

I. INTRODUCTION

The artificial left-handed metamaterials (LHMs), which have many exotic properties that cannot be found in the natural materials, are now extensively studied by many groups. In a theoretical work, Veselago [1] named left-handed metamaterials for such media, the electric, magnetic, and wave-vector components of the electromagnetic wave (EM wave) form a left-handed coordinate system. He also predicted that the media exhibit negative refractive index when it simultaneously has negative permittivity ($\varepsilon<0$) and negative permeability ($\mu<0$) and investigated other interesting properties of the LHMs such as reversal of the Doppler effects, backward Cherenkov radiation, and so on. These results have not attracted much attention in a long period for the absence of LHMs in nature. After about 30 years, Pendry *et al.* [2,3] proposed that the arrays of the continuous metallic rods and the metallic split-ring resonators (SRRs) can exhibit negative permittivity and negative permeability, respectively. In the year 2000, Smith *et al.* [4] constructed the first LHM in the world based on the idea of Pendry by arranging the arrays of Rods and SRRs alternately. Then their findings light the flame of studying LHMs.

In recent years after Smith *et al.* [4] constructed the first LHM, many groups [5–8] further supported the existence of the negative refraction numerically and experimentally and investigated other phenomena of the LHMs such as bianisotropic [9–12] and so on. Besides those SRR and Rod structural left-handed metamaterials, some novel types of left-handed metamaterials are proposed such as Ω-shaped [13], S-shaped [14], H-shaped [15], cut wires [16], fishnet structure [17], and so on. These new types of metamaterials exhibit simultaneous negative electric response and negative magnetic response in a certain frequency range with the fixed polarization of the incident EM wave. For planar left-handed metamaterials, we can divide them into two types: the parallel incidence case [13,14,18–22] (the electromagnetic wave incident parallel to the plane of the cell) and the normal-incidence case [15–17,23–34] (the electromagnetic wave incident normal to the plane of the cell) based on the propagation directions of the incident EM wave.

In order to reduce the effect of EM wave propagation direction on the metamaterial's response, in this paper, we proposed a high-symmetric fourfold C-shaped planar left-handed metamaterial. It can exhibit negative refractive index with EM wave incident in both the parallel and normal directions.

II. NUMERICAL ANALYSIS

A. Structural model

The unit cell of the fourfold C-shaped left-handed metamaterial is shown in Fig. 1, where the 0.035-mm-thickness copper wires are printed on both sides of the substrate symmetrically (in the simulations of this paper, we select FR-4 as the substrate with the relative dielectric constant $\varepsilon_r=4.4$ and the conductivity $\sigma=0.02$ S/m, respectively), and other dimensions are displayed in the caption under Fig. 1. In constructing the slab of the metamaterial, the

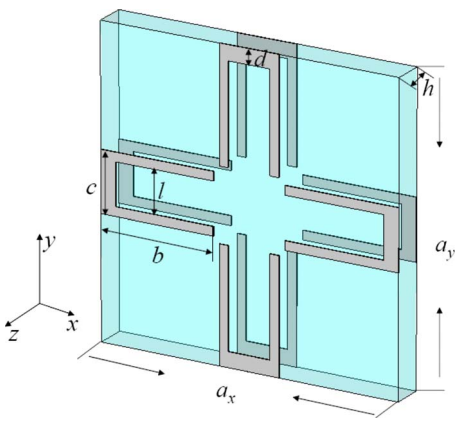

FIG. 1. (Color online) The unit cell of the fourfold C-shaped metamaterial with the geometric dimensions $a_x=a_y=10$ mm, $b=3.8$ mm, $c=2$ mm, $d=0.5$ mm, $h=1$ mm, and $l=1.4$ mm.

*lvjianhong@smail.hust.edu.cn
†xwhu@mail.hust.edu.cn

elementary cells are periodically repeated along the x, y, and z directions with constants of 10 mm, 10 mm, and 3 mm, respectively.

For this high-symmetric fourfold C-shaped planar metamaterial, there are six polarization cases with the EM wave propagating along three different directions (in the x, y, and z directions, respectively). Among these six cases, there are two polarization cases that cannot exhibit left-handed behavior with the electric field perpendicular to the plane, and we will not consider these two cases in this paper. For other four polarization cases, two are parallel incidence cases while the other two cases are normal incidence. Taking into consideration the isotropic xy plane, we can only calculate two polarization cases, as, for example, one is the parallel incidence case ($\mathbf{k}\|x$) with the electric and magnetic field along the y ($\mathbf{E}\|y$) and z ($\mathbf{H}\|z$) directions, and another one is the normal-incidence case ($\mathbf{k}\|z$) with the electric and magnetic fields along the y ($\mathbf{E}\|y$) and x ($\mathbf{H}\|x$) directions, respectively.

The mechanisms of the negative refraction of two incidence cases are different. For the normal-incidence case, which we will study in detail in the next part (Sec. II B), the high-symmetric fourfold C-shaped metamaterial works like the fishnet structure. For the parallel incidence case, the metamaterial works like the cut wire and SRRs structure, and it will be studied in Sec. II C. In Sec. II D, the different electric responses of the normal and parallel incidence cases to the incident electromagnetic wave are discussed and compared.

B. Normal-incidence case

For the normal-incidence case, we take the polarization that the electric and magnetic fields along the y and x directions as an example to verify the left-handed properties of the metamaterial, which we have pointed out above. Under this polarization, we simulate the unit cell of fourfold C-shaped metamaterial by the software CST MICROWAVE STUDIO and obtain the effective constitutive parameters from retrieving [35,36] the simulated scattering parameters [the reflection (S_{11}) and transmission (S_{21}) data]. In the simulation, we have open boundary along the propagation direction and periodic boundaries along the lateral directions.

The effective constitutive parameters impedance Z, permittivity ε, permeability μ, and refractive index n are plotted in Figs. 2(a)–2(d), where the solid and dashed lines denote the real and imaginary parts of the effective parameters, respectively. From Fig. 2, we find that the high-symmetric fourfold C-shaped metamaterial can exhibit negative refractive index in a narrow frequency range (10.15–10.3 GHz) with simultaneous negative permittivity and negative permeability.

Furthermore, the transmission of the planar metamaterial is simulated with five unit cells along the propagation direction, and the result is shown in Fig. 3. From Fig. 3, we obtain that the metamaterial exhibit a left-handed transmission pass band in the frequency range of about 10–10.5 GHz. This left-handed transmission pass band (0.5 GHz) is much wider than the retrieved left-handed frequency band (0.15 GHz), it

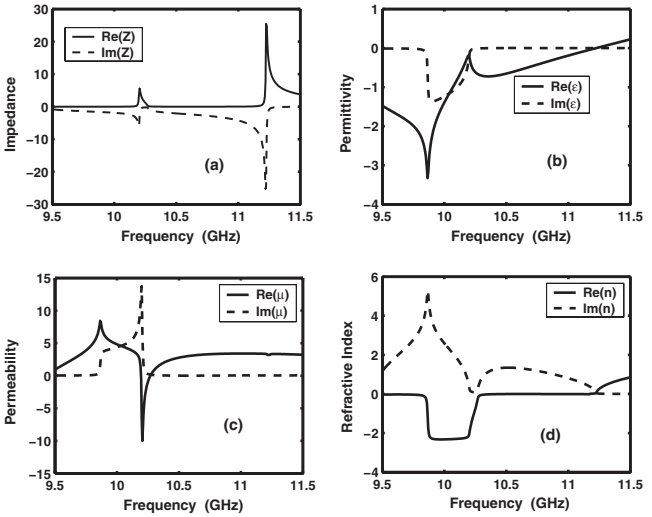

FIG. 2. The retrieved effective constitutive parameters of the normal-incidence case: (a) impedance Z, (b) permittivity ε, (c) permeability μ, and (d) refractive index n. The solid and dashed lines denote the real and imaginary parts of the effective parameters, respectively.

may be due to the coupling between the layers that we have not considered in retrieving the unit cell. The low left-handed transmission (−15 dB) of metamaterial is mainly due to losses in the dielectric substrates between the metallic wires, so we can use low-loss substrates instead of high-loss substrates to reduce the transmission loss, and other methods to reduce losses of left-handed metamaterial can be found in Ref. [37], which have been discussed by Zhou *et al.*

As mentioned above, the mechanism of negative refraction of the normal-incidence case is similar to the fishnet structure [17]. Along the electric field direction, the resemble cut-wires structure have an electric response to the EM wave and then exhibit a negative permittivity within a certain frequency range. Meanwhile, the induced opposite direction currents in the metallic wires of the opposite sides of the

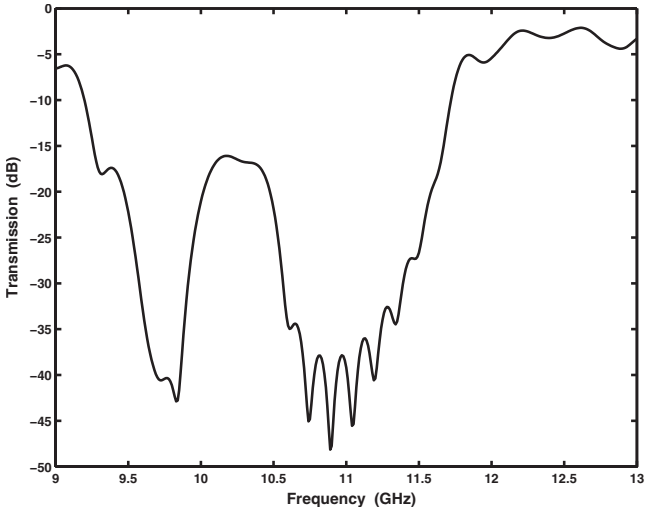

FIG. 3. Transmission of the normal-incidence case with five layers stacked along the propagating direction.

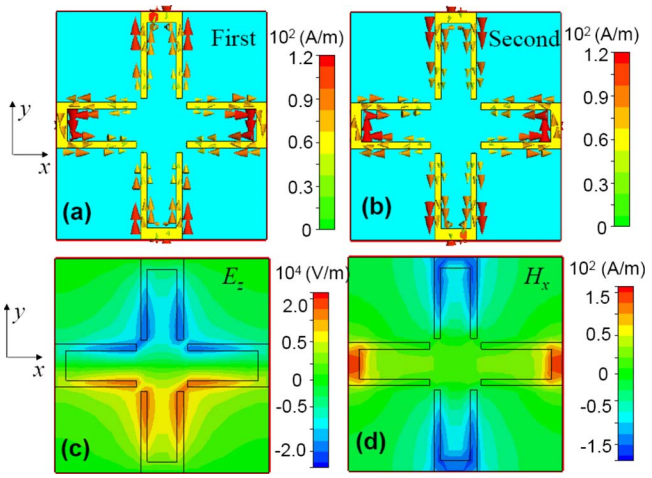

FIG. 4. (Color online) Current distributions of two sides: (a) the first side and (b) the second side of the unit cell, and the dominant components of (c) the electric and (d) magnetic fields of the normal-incidence case at the frequency just above the magnetic resonance.

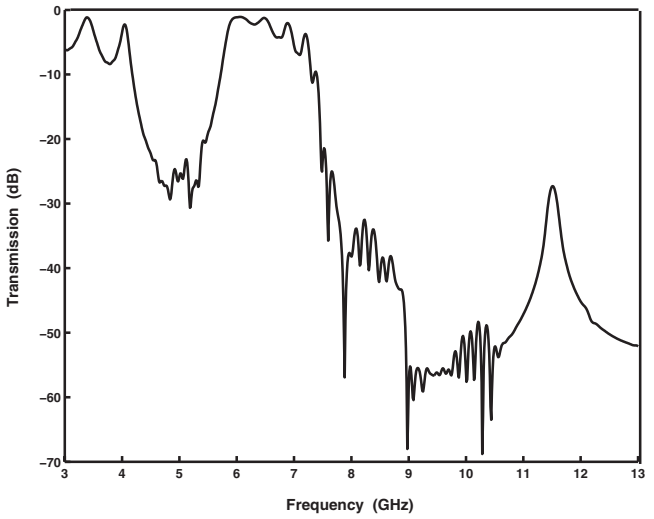

FIG. 5. The transmission of the array of the high-symmetric fourfold C-shaped metamaterial for the parallel incidence case.

substrates form a current loop and exhibit a self-inductance (L). Together with the capacitance (C) between the opposite metallic wires, the fourfold C-shaped resonator works like a LC resonant circuit and then exhibit a negative magnetic resonance. Therefore, the metamaterial exhibit a negative refractive index when the negative electric and magnetic responses are overlapped.

To understand the discussion above clearly, we display the distribution of the currents in the metallic wires of both sides and the main components of the electric (E_z) and magnetic fields (H_x) in Figs. 4(a)–4(d). From the distribution of the currents and fields as shown in Fig. 4, we find that they are very similar to the case of the fishnet structure as shown in Figs. 7 and 8 in Ref. [17]. The currents of two sides [the first and second sides as shown in Figs. 4(a) and 4(b)] are opposite to each other and, for either side (the first or the second side), the currents at the neck regions (in the unit cell as shown in Fig. 1, we define the up and down fold parts as the neck regions corresponding to the fishnet structure) are opposite to the currents at the slab regions (as defining the neck regions, we define the left and right fold parts as the slab regions). These opposite currents of the neck and slab regions make the strong charges accumulating around the gaps and then produce strong electric fields between the metallic wires of two sides as shown in Fig. 4(c). Furthermore, the current loops formed by the opposite currents of two sides produce magnetic fields as shown in Fig. 4(d), and the induced magnetic fields at the neck regions are opposite to the slab regions; it is due to the opposite currents at the neck and slab regions. After further analyzing the distribution of the fields, the magnetic resonant frequency and the magnetic plasma frequency can be calculated by using the equivalent LC circuit theory as discussed in Ref. [17], and we will not discuss it here.

C. Parallel incidence case

In order to exhibit left-handed properties with the parallel incident EM wave, we only need to fix the magnetic field perpendicular to the substrates ($\mathbf{H} \| z$). As mentioned in Sec. II A, we take the polarization with the wave vector and the electric field along the x and y directions, respectively.

For the fourfold C-shaped metamaterial, it is actually a bianisotropic medium for the coupling between its electric and magnetic responses. So it is complex and difficult to obtain the effective constitutive parameters from the general retrieval method [35,36]. To demonstrate the left-handed properties of the parallel incidence case, we first simulate the transmission of the array of the fourfold C-shaped metamaterial, which have N_x=6, N_y=3, and N_z=6 unit cells, and periodically arranged in the x, y, and z directions with the constants of 10 mm, 10 mm, and 3 mm, respectively. The simulated transmission result is plotted in Fig. 5. From Fig. 5, we find that the metamaterial exhibit a pass band in the frequency range of about 5.6–7.6 GHz. But so far, we cannot be sure whether this pass band is a left-handed pass band or not.

To further verify the refractive behavior of the metamaterial, we simulate the refractive direction of the electromagnetic wave through a wedge shape slab of the metamaterial by the software ANSOFT HFSS at three different frequencies. The numerical results are shown in Figs. 6(a)–6(c). This method has been used in some earlier articles [38,39], and it can display a direct image of the negative refraction behavior. In this wedge, the refraction interface has a staircase pattern with one unit cell step in both x and y directions and has six unit cells arrayed along both x and y directions, respectively. The wedge is positioned between two magnetic conducting plates (perfect magnetic boundaries) to form a two-dimensional waveguide, and the spacing between the two plates is 3 mm (one unit cell). An electromagnetic wave is guided by the rectangular channel and incident on the first interface of the wedge normally. After it propagates through the wedge, the wave will undergo refraction at the second interface. Figures 6(a)–6(c) illustrate the magnitude distribution of the magnetic field at three frequencies of 6 GHz, 6.4 GHz, and 7 GHz of the incident EM wave, respectively. The solid arrow lines denote the transmission direction of the

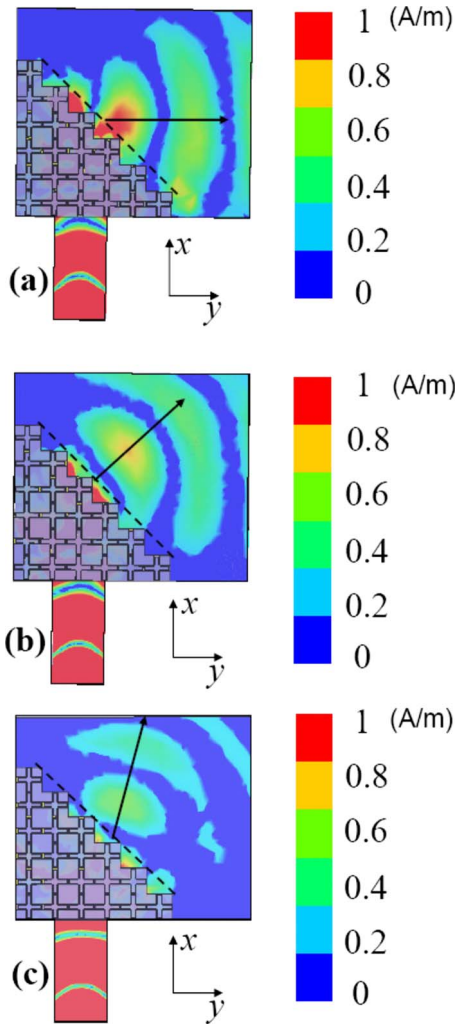

FIG. 6. (Color online) Magnitude distributions of the magnetic field of the refractive wave for the parallel incidence case at frequency of (a) 6 GHz, (b) 6.4 GHz, and (c) 7 GHz, respectively.

refracted wave. From Figs. 6(a)–6(c), we can obviously find that the refracted wave have negative, zero, and positive refractive indexes at the frequencies of 6.0 GHz, 6.4 GHz, and 7.0 GHz, respectively. So the high-symmetric fourfold C-shaped metamaterial is a negative-zero-positive metamaterial [40,41] for the parallel incidence case, and it can exhibit left-handed properties in a certain frequency range of about 5.6–6.4 GHz.

To understand the metamaterial's response to the EM wave for the parallel incidence case, we first display the distributions of the current in the metallic wires, the dominant components of the electric (E_x) and magnetic field (H_z) in Figs. 7(a)–7(c) as the normal-incidence case. Under the parallel incident EM wave, the charges are accumulated to the gaps and produce a capacitance (C) in each gap as shown in Fig. 7(b). Furthermore, the magnetoinductive current [as shown in Fig. 7(a)], which circled the fourfold C-shaped resonator, produce an antiparallel magnetic field [as shown in Fig. 7(c)] with respect to the magnetic field of the EM wave and exhibit a self-inductance (L). This inductance combines with the capacitances in the gaps forming a LC resonant

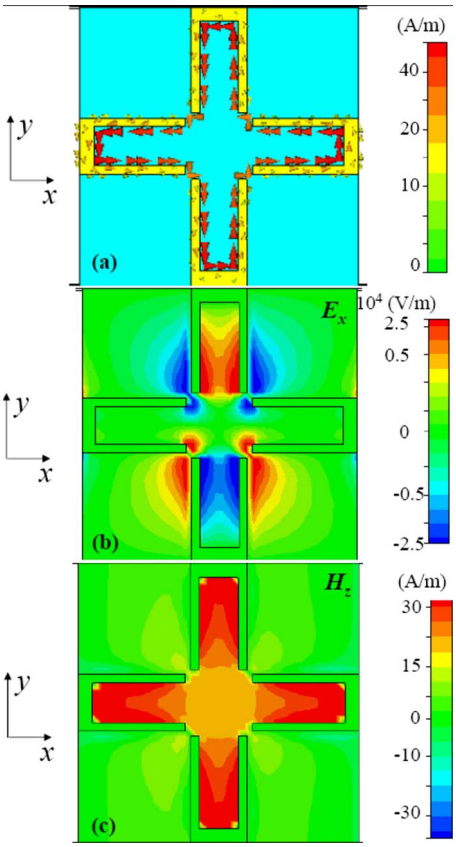

FIG. 7. (Color online) Magnitude distributions of the current (a), the dominant components of the electric field (b), and the magnetic field (c) of the parallel incidence case at the frequency just above the magnetic resonance.

circuit and then exhibits a negative magnetic response. Overlapped with the negative electric response of this resemble cut-wire structure, the metamaterial exhibits left-handed properties for the parallel incidence case.

D. Different electric responses of two incidence cases

For both the normal and parallel incidence cases, though the electric fields of the EM wave are always parallel along the metallic wires, the electric responses are different. To explain the different electric responses, we simulate the transmissions of the metamaterial for both the normal and parallel incidence cases, and the transmission of array of the simplified equivalent cut wires (the unit cell of the equivalent cut wire is shown in the inset of Fig. 8) is also simulated to be compared with. From the simulated transmission results as shown in Fig. 8, we obtain that the array of the simplified equivalent cut wires exhibits a negative electric response in the frequency range of 3.0–12.0 GHz. For the high-symmetric fourfold C-shaped metamaterial, it exhibits a negative electric response within the frequency range of 9.0–11.7 GHz of the normal-incidence case, while it exhibits a negative electric response within the frequency range of 4.0–6.4 GHz of the parallel incidence case.

Compared with the electric response of the simplified equivalent cut wires, we find that the electric plasma fre-

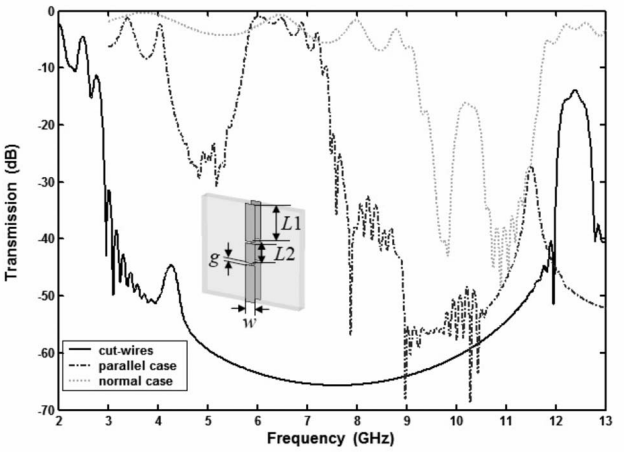

FIG. 8. The transmission (solid line) of array of the simplified equivalent cut wires (the unit cell is shown in the inset), and the transmissions of the planar left-handed metamaterial for the normal (dotted line) and the parallel (dashed-dotted line) incidence cases, respectively. For the unit cell of the simplified equivalent cut wires, as shown in the inset, the geometric dimensions are equivalently obtained from the sizes of the unit cell of the fourfold C-shaped metamaterial as shown in Fig. 1, $L1=b=3.8$ mm, $L2=c=2.0$ mm, $w=2d=1.0$ mm, and $g=(a\text{-}2b\text{-}c)/2=0.2$ mm, respectively.

quency (ω_p) of the parallel incidence case shifts to a lower effective plasma frequency ($\omega_p'=6.4$ GHz), and the electric resonant frequency (ω_e) of the normal-incidence case shifts to a higher frequency ($\omega_e'=9.0$ GHz). The shifts of above frequencies are due to the different distribution of the induced currents in the metallic wires. For the parallel incidence case, the fourfold C-shaped resonator which circled with a magnetic-induced current, exhibits an electric response. Then this electric response is coupled to the electric response of the resemble cut-wire structure, and makes the electric plasma frequency (ω_p) of the structure shift to a lower effective plasma frequency ($\omega_p'=6.4$ GHz). Different from the parallel incidence and the equivalent cut-wires cases, the neck and slab regions of the fourfold C-shaped structure have opposite currents under the normal incident EM wave, and it exhibits a different electric response. Therefore, for the normal-incidence case, the electric resonant frequency (ω_e) is shift to a higher value ($\omega_e'=9.0$ GHz).

Furthermore, from Fig. 8, we find that the values of the electric plasma frequency of two incidence cases are nearly equal to each other (about 11.7 GHz); it is because the electric plasma frequency (ω_p) is only dependent on the geometric sizes of the structures. For the simplified equivalent cut wires, its electric response is a little different from the fourfold C-shaped left-handed metamaterial. From Fig. 8, we can find that the electric plasma frequency (ω_p) of the equivalent cut wires (12 GHz) is a little larger than the fourfold C-shaped metamaterial (11.7 GHz), and the electric resonant frequency (ω_e) of the equivalent cut wires is shifted to a lower frequency (3 GHz). These differences are due to the errors in the process of the simplification. Though the electric response of the simplified equivalent cut wires is a little different from the fourfold C-shaped left-handed metamaterial, it can help to quantitatively explain the different electric responses of two incidence cases.

III. CONCLUSIONS

In conclusion, we report a left-handed metamaterial with fourfold C-shaped rings symmetrically printed on both sides of the substrates. This planar metamaterial can exhibit a left-handed behavior with simultaneous normal and parallel incidences. For different incidence cases, the negative refraction pass bands are different; it exhibits a negative refraction pass band in the frequency range of 10.0–10.5 GHz of the normal-incidence case, while it exhibits a negative refraction pass band in the frequency range of 5.6–6.4 GHz of the parallel incidence case. Furthermore, the different electric responses of two incidence cases are discussed, and it is due to the different distribution of the induced currents in the metallic wires. The simulated results verify the above conclusions perfectly. Lastly, this stacked layer-by-layer planar left-handed metamaterial no need to intercross the substrates to each other, so it can be easily realized, and it will play an important role in constructing the high-dimensional metamaterial.

ACKNOWLEDGMENT

This work was supported by the National Natural Science Foundation of China under Contract No. 10775055.

[1] V. G. Veselago, Sov. Phys. Usp. **10**, 509 (1968).
[2] J. B. Pendry, A. J. Holden, W. J. Stewart, and I. Youngs, Phys. Rev. Lett. **76**, 4773 (1996).
[3] J. B. Pendry, A. J. Holden, D. J. Robbins, and W. J. Stewart, IEEE Trans. Microwave Theory Tech. **47**, 2075 (1999).
[4] D. R. Smith, W. J. Padilla, D. C. Vier, S. C. Nemat-Nasser, and S. Schultz, Phys. Rev. Lett. **84**, 4184 (2000).
[5] R. A. Shelby, D. R. Smith, and S. Schultz, Science **292**, 77 (2001).
[6] J. A. Kong, B.-I. Wu, and Y. Zhang, Appl. Phys. Lett. **80**, 2084 (2002).
[7] C. G. Parazzoli, R. B. Greegor, K. Li, B. E. C. Koltenbah, and M. Tanielian, Phys. Rev. Lett. **90**, 107401 (2003).
[8] L. Ran, J. Huangfu, H. Chen, X. Zhang, K. Chen, T. M. Grzegoczyk, and J. A. Kong, J. Appl. Phys. **95**, 2238 (2004).
[9] R. Marques, F. Medina, and R. Rafii-E1-Idrissi, Phys. Rev. B **65**, 144440 (2002).
[10] N. Katsarakis, T. Koschny, M. Kafesaki, E. N. Economou, and C. M. Soukoulis, Appl. Phys. Lett. **84**, 2943 (2004).
[11] D. R. Smith, J. Gollub, J. J. Mock, W. J. Padilla, and D. Schurig, J. Appl. Phys. **100**, 024507 (2006).
[12] K. Aydin, Z. Li, M. Hudlicka, S. A. Tretyakov, and E. Ozbay, New J. Phys. **9**, 326 (2007).
[13] J. Huangfu, L. Ran, H. Chen, X. Zhang, K. Chen, T. M. Grzegoczyk, and J. A. Kong, Appl. Phys. Lett. **84**, 1537 (2004).
[14] H. Chen, L. Ran, J. Huangfu, X. Zhang, K. Chen, T. M. Grze-

gorczyk, and J. A. Kong, Phys. Rev. E **70**, 057605 (2004).
[15] J. Zhou, T. Koschny, L. Zhang, G. Tuttle, and C. M. Soukoulis, Appl. Phys. Lett. **88**, 221103 (2006).
[16] J. Zhou, L. Zhang, G. Tuttle, T. Koschny, and C. M. Soukoulis, Phys. Rev. B **73**, 041101(R) (2006).
[17] M. Kafesaki, I. Tsiapa, N. Katsarakis, Th. Koschny, C. M. Soukoulis, and E. N. Economou, Phys. Rev. B **75**, 235114 (2007).
[18] T. Koschny, M. Kafesaki, E. N. Economou, and C. M. Soukoulis, Phys. Rev. Lett. **93**, 107402 (2004).
[19] K. Aydin, K. Guven, M. Kafesaki, L. Zhang, C. M. Soukoulis, and E. Ozbay, Opt. Lett. **29**, 2623 (2004).
[20] T. M. Grzegoczyk, C. D. Moss, J. Lu, X. Chen, J. Pacheco, and J. A. Kong, IEEE Trans. Microwave Theory Tech. **53**, 2956 (2005).
[21] K. Aydin, K. Guven, C. M. Soukoulis, and E. Ozbay, Appl. Phys. Lett. **86**, 124102 (2005).
[22] E. Ozbay, K. Aydin, and K. Guven, J. Opt. A, Pure Appl. Opt. **9**, S301 (2007).
[23] S. Zhang, W. Fan, N. C. Panoiu, K. J. Malloy, R. M. Osgood, and S. R. J. Brueck, Phys. Rev. Lett. **95**, 137404 (2005).
[24] S. Zhang, W. Fan, K. J. Malloy, S. R. J. Brueck, N. C. Panoiu, and R. M. Osgood, Opt. Express **13**, 4922 (2005).
[25] V. M. Shalaev, W. Cai, U. K. Chettiar, H. K. Yuan, A. K. Sarychev, V. P. Drachev, and A. V. Kildishev, Opt. Lett. **30**, 3356 (2005).
[26] G. Dolling, C. Enkrich, M. Wegener, C. M. Soukoulis, and S. Linden, Science **312**, 892 (2006).
[27] G. Dolling, C. Enkrich, M. Wegener, C. M. Soukoulis, and S. Linden, Opt. Lett. **31**, 1800 (2006).
[28] K. Guven, M. D. Caliskan, and E. Ozbay, Opt. Express **14**, 8685 (2006).
[29] J. Zhou, E. N. Economon, T. Koschny, and C. M. Soukoulis, Opt. Lett. **31**, 3620 (2006).
[30] C. Imhof and R. Zengerle, Opt. Express **14**, 8257 (2006).
[31] G. Dolling, M. Wegener, C. M. Soukoulis, and S. Linden, Opt. Lett. **32**, 53 (2007).
[32] K. Guven, A. O. Cakmak, M. D. Caliskan, T. F. Gundogdu, M. Kafesaki, C. M. Soukoulis, and E. Ozbay, J. Opt. A, Pure Appl. Opt. **9**, S361 (2007).
[33] G. Dolling, M. Vegener, and S. Liden, Opt. Lett. **32**, 551 (2007).
[34] J. Valentine, S. Zhang, T. Zentgraf, E. Ulin-Avila, D. A. Genov, G. Bartal, and X. Zhang, Nature (London) **455**, 376 (2008).
[35] X. Chen, T. M. Grzegorczyk, B.-I. Wu, J. Pacheco, and J. A. Kong, Phys. Rev. E **70**, 016608 (2004).
[36] D. R. Smith, D. C. Vier, Th. Koschny, and C. M. Soukoulis, Phys. Rev. E **71**, 036617 (2005).
[37] J. Zhou, T. Koschny, and C. M. Soukoulis, Opt. Express **16**, 11147 (2008).
[38] P. Kolinko and D. R. Smith, Opt. Express **11**, 640 (2003).
[39] Z. G. Dong, S. N. Zhu, H. Liu, J. Zhu, and W. Cao, Phys. Rev. E **72**, 016607 (2005).
[40] F. Zhang, G. Houzet, E. Lheurette, D. Lippens, M. Chaubet, and X. Zhao, J. Appl. Phys. **103**, 084312 (2008).
[41] J. Lv, B. Yan, M. Liu, and X. Hu, Phys. Rev. E **79**, 017601 (2009).